Available online at www.sciencedirect.com
SCIENCE DIRECT®
Chemistry and Physics of Lipids 138 (2005) 60–68
CPL
CHEMISTRY AND PHYSICS OF LIPIDS
www.elsevier.com/locate/chemphyslip

Regio- and stereoselective oxidation of linoleic acid bound to serum albumin: identification by ESI–mass spectrometry and NMR of the oxidation products

Claire Dufour *, Michèle Loonis

Institut National de la Recherche Agronomique, UMR A408, Safety and Quality of Plant Products, Agroparc, 84914 Avignon Cedex 9, France

Received 24 May 2005; received in revised form 5 August 2005; accepted 17 August 2005
Available online 12 September 2005

Abstract

An efficient RP-HPLC method was developed for the detection of the oxidation products derived from the AAPH-initiated peroxidation of linoleic acid bound to human serum albumin. Diode array UV-detection allowed the quantification at 234 nm of four regioisomeric hydroperoxyoctadecadienoic acids (HPODE) and four hydroxyoctadecadienoic acids (HODE) while at 280 nm four oxooctadecadienoic acid isomers (KODE) were detected. Full identification of the different underivatized HODE, HPODE and KODE isomers was achieved by negative ESI–mass spectrometry outlining common fragmentation pathways for 9- and 13-regioisomers. Chemical synthesis of 9-(*E*,*Z*)-, 9-(*E*,*E*)-, 13-(*Z*,*E*)- and 13-(*E*,*E*)-KODE helped to their structural characterization by ^{1}H NMR. Lipid peroxidation in the presence of albumin proved to be regioselective with a larger accumulation of 13-HPODE and 9-KODE isomers. Thermodynamically more stable *E*,*E*-stereoisomers were also favored by albumin for both HPODE and KODE.

Keywords: Hydroperoxyoctadecadienoic acid; Oxooctadecadienoic acid; Hydroxyoctadecadienoic acid; Lipid peroxidation; Electrospray ionization–mass spectrometry; NMR

1. Introduction

For a long time, lipid peroxidation has been considered as a deleterious process leading to atherogenic LDL or membrane disruption. However, when cell-mediated, lipid peroxidation is a normal physiological process with involvement in eicosanoid synthesis or cell maturation (Kuhn and Borchert, 2002). Lipoxygenase-catalyzed lipid peroxidation which can be up- and downregulated is well adapted to the above biological requirements whereas lipid autoxidation resulting from pathological events may escape metabolic control leading thus to harmful side effects.

Although both reactions with linoleic acid lead to hydroperoxyoctadecadienoic acids as primary oxidation products, only lipoxygenases (LOX) display positional and stereospecificities. For example, soybean LOX catalyzes the conversion of linoleic acid into 13(*S*)-hydroperoxy-(9*Z*,11*E*)-octadecadienoic acid

Abbreviations: HODE, hydroxyoctadecadienoic acid; HPODE, hydroperoxyoctadecadienoic acid; KODE, oxooctadecadienoic acid; LH, linoleic acid

* Corresponding author. Tel.: +33 4 32 72 25 15; fax: +33 4 32 72 24 92.
E-mail address: cdufour@avignon.inra.fr (C. Dufour).

0009-3084/$ – see front matter © 2005 Elsevier Ireland Ltd. All rights reserved.
doi:10.1016/j.chemphyslip.2005.08.003

while tomato or corn seed LOX preferentially produce 9(*S*)-hydroperoxy-(10*E*,12*Z*)-octadecadienoic acid (Hamberg, 1971; Matthew et al., 1997; Gardner and Grove, 2001). In autoxidation, however, both *EZ* and *EE* stereoisomers are formed with the double bond closer to the oxygenated center being *E* (Chan and Levett, 1977). Usually, these unstable hydroperoxides (HPODE) decay to secondary oxidation products, identified mainly as hydroxy- (HODE), epoxyhydroxy- and oxo-derivatives (KODE) and dependent on the presence of factors such as metal ions or reducing agents (Spiteller and Spiteller, 1998; Dix and Marnett, 1985).

The separation of the linoleic acid oxidation products is usually challenged by chromatographic means. Normal-phase HPLC has been widely used for the tentative separation of either native HODE, HPODE and KODE (Wu et al., 1995) or the corresponding methyl esters derivatives (Hilbers et al., 1996). Reverse-phase HPLC may appear less efficient (Pérez Gilabert and Garcia Carmona, 2002; Banni et al., 1996).

Structural informations on the peroxidation products such as mass data and position of the oxygenated center are gained by mass spectrometry. Gas chromatography–mass spectrometry (GC–MS) usually requires derivatization of the polar lipid derivatives before injection (Spiteller and Spiteller, 2000). Furthermore, analysis of intact hydroperoxides by GC–MS is impeded by their thermal instability (Pérez Gilabert and Garcia Carmona, 2002). Development of soft ionization techniques such as electrospray has allowed the detection of molecular ions of native oxidation products (Iwase et al., 1998). The state of the art in this area is brought by tandem mass spectrometry as shown by applications to fatty acid oxygenation products (Bylund et al., 1998; Kerwin and Torvik, 1996; MacMillan and Murphy, 1995; Schneider et al., 1997). However, such an equipment is not routinely available in laboratories supporting the development of simpler but as efficient methods in LC–MS.

Our interest in the inhibition of plasma lipid peroxidation by bioavailable secondary metabolites led us to study a biologically-relevant plasma model chiefly constituted by linoleic acid and albumin. A reverse-phase HPLC method was thus developed to quantify simultaneously the resulting lipid oxidation products and the antioxidants. Full identification of the different underivatized HODE, HPODE and KODE isomers was achieved by mass spectrometry in combination with electrospray ionization. Assignment was further assisted by chemical synthesis and NMR analysis of the different KODE. The regio- and stereoselectivities for the peroxidation of HSA-bound linoleic acid were also established.

2. Experimental

2.1. Chemicals

Fatty acid-free human serum albumin (HSA, A 1887), linoleic acid (LH), 13(*S*)-hydroperoxy-(9*Z*,11*E*)-octadecadienoic acid, 13(*S*)-hydroxy-(9*Z*,11*E*)-octadecadienoic acid, 2,2′-azobis(2-amidinopropane) hydrochloride (AAPH) and sodium dihydrogenphosphate were used as received from Sigma–Aldrich (St. Quentin Fallavier, France). Phosphate buffer (pH 7.4, 50 mM NaH_2PO_4, 100 mM NaCl) was prepared in Millipore Q-Plus water and stirred with a chelating resin (Chelex 100, 0.4 mequiv./mM, BioRad). MeOH and CH_3CN were of HPLC grade.

2.2. Lipid peroxidation

Linoleic acid (100 μL, 200 mM in MeOH) was added via syringe to albumin in buffer (10 mL to 33 g/L) followed by solid AAPH (82 mg). The reaction mixture was stirred in an oven at 37 °C. Aliquots (0.5 mL) were removed, acidified with an equal volume of 0.05 N HCl and extracted three times with 1 mL of ethyl acetate/hexane (1:1). The organic phase was washed with a saturated NaCl solution, dried over Na_2SO_4, concentrated under N_2 and taken up in acetone before freezing. The extraction yields were evaluated by spiking directly albumin with linoleic acid (66%), HODE and HPODE (84%) and KODE (88%) ($n = 3$).

2.3. HPLC and HPLC/MS analyses of lipid peroxidation products

Lipid peroxidation products were separated by RP-HPLC coupled to Diode Array Detection (Hewlett-Packard 1100) using a Alltima C18 column (5 μm, 150 mm × 4.6 mm, Alltech) equipped with a Alltima C18 guard column (5 μm) (flow rate = 1 mL/min, $T = 35$ °C, volume injected = 10 μL). The solvent system was a gradient of A (0.05% HCOOH in H_2O) and B (CH_3CN) with 50% B from 0 to 5 min, 60% B at 15 min, 73% B at 30 min and 100% B at 40 min. HPODE and HODE were detected at 234 nm, KODE at 280 nm and LH at 210 nm. Structure determination was performed by HPLC–MS (Plateform LCZ, Micromass, coupled to a HP 1050, see HPLC analysis for the conditions of elution) in the negative electrospray ionization mode (cone voltage = 30 and 50 V, nitrogen flow = 3.2 L/h, source block and desolvation temperatures = 150 and 250 °C, respectively, flow rate

into the source = 50 μL/min). Authentic standards of 13(*S*)-hydroperoxy-(9*Z*,11*E*)-octadecadienoic acid and 13(*S*)-hydroxy-(9*Z*,11*E*)-octadecadienoic acid as well as synthetic KODE samples were used for co-injection and calibration curves (five point measurements) of total, respectively, HPODE, HODE and KODE. Micromolar solutions gave areas of 11 for HPODE and HODE, 2 for KODE and 2 for LH ($n = 3$ and $r2 > 0.999$).

2.4. Ketodiene synthesis and NMR analysis

From HODE. Neat linoleic acid (1.19 g) was left to autoxidize at room temperature for a week. The mixture containing LH and the HPODE in ethanol (35 mL) was reduced with sodium borohydride (106 mg) at 0 °C, hydrolyzed with water (35 mL), acidified to pH 3 with 1 N HCl and extracted three times with hexane/ethyl acetate (1:1). The organic extracts were washed with sat. NaCl, dried over Na_2SO_4 and concentrated in vacuo. Silica gel chromatography (eluent: ethyl acetate/hexane 2:8) yielded four fractions enriched in the different HODE (156 mg, 12.5% overall yield) and used for mass analysis. Oxidation of the respective fractions by pyridinium dichromate (PDC) helped to the chromatographic assignment of the HODE. For example, HODE3 (28 mg) was oxidized with PDC (50 mg) in chloroform (4 mL) at 0 °C. PDC was precipitated with Et_2O (8 mL) and the solution eluted over silica gel (ethyl acetate/Et_2O 6:4) to yield quantitatively KODE4.

From HPODE. Pure HPODE were obtained by autoxidation of neat linoleic acid followed by gel chromatography on silica gel (ethyl acetate/hexane, 5:95). The HPODE (25 mg) were then treated with pyridine (1.75 mL) and acetyl chloride (63.5 μL) to yield directly the corresponding KODE (16.7 mg, 71% yield) (Porter and Wujek, 1987). The fraction containing the KODE was analyzed in HPLC/MS and next purified by semi-preparative HPLC (Waters 600) coupled to a UV detection (Waters 486) using a Uptisphere ODB column (10 μm, 250 mm × 21.2 mm) equipped with a Uptisphere ODB guard column (5 μm, 33 mm × 21.2 mm) (flow rate = 18 mL/min, $T = 35$ °C, volume injected = 500 μL). The solvent system was a gradient of A (0.05% HCOOH in H_2O) and B (CH_3CN) with 65% B from 0 to 5 min, 70% B at 10 min, 73% B from 15 to 25 min and 80% B at 35 min. Four fractions were obtained containing each a major KODE (purity 85–95%). ^{1}H NMR spectra were obtained with a cryoprobe on a Bruker DRX-500 in CDCl3 (300 K) with $CHCl_3$ as the internal reference at 7.26 ppm.

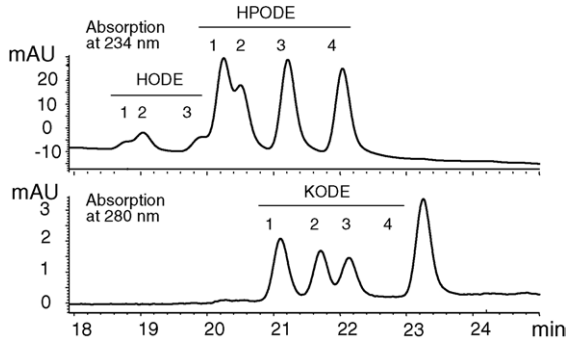

Fig. 1. HPLC chromatogram after 7 h of peroxidation for linoleic acid bound to human serum albumin.

3. Results

The HPLC chromatogram obtained for LH autoxidation in the 18–24 min area is qualitatively similar to the one obtained for chemical oxidation of HSA-bound LH except that HPODE are major compounds in autoxidation (Fig. 1). Chemical synthesis of HODE and KODE from HPODE produced by autoxidation was used to assess the structures of the oxidation products obtained in the presence of HSA. Solvent and gradient conditions in HPLC were refined until well-separated peaks were obtained for each product. Each oxidation product is numbered according to the LC peak from which it originates.

3.1. Structures of the HPODE products

Mass analysis was conducted at low and high voltages in order to get either the molecular ion or full fragmentation for structural assignment. Product ions and abundances are reported for the latter conditions in Table 1. Although no sodium-based chemical was used for HPODE purification and HPLC analysis, ions detected at *m*/*z* 333 and 315 suggest the presence of sodium in the parent ions $[M + Na - 2H]^-$ and the dehydrated parent ions $[M + Na - H_2O - 2H]^-$. Abundant ions at *m*/*z* 293 resulted from the loss of water and proved to be major for HPODE2 and 4. The expected loss of H_2O_2 did not appear as a degradation pathway and decarboxylation of the fatty acids was the next step. Other cleavages were characteristic of the 9- and 13-oxygenation of the primary oxidation products. Similar patterns in the product ion spectra were displayed for HPODE1 and 3. The product ion at *m*/*z* 223 resulted from cleavage between C13 and C14. Subsequent losses of CO and CO_2 yielded ions at *m*/*z* 195 and 179 while the most abundant ion was detected at *m*/*z* 113. HPODE1 and 3 are thus

Table 1
Product ions (*m*/*z*) and proposed structures for fragments issued from hydroperoxyoctadecadienoic acids (HPODE) in ESI–MS[a]

	HPODE1 13-*Z*,*E*-HPODE	HPODE2 9-*E*,*Z*-HPODE	HPODE3 13-*E*,*E*-HPODE	HPODE4 9-*E*,*E*-HPODE
$[M + Na - 2H]^-$	333 (2)	333 (4)	333 (5)	333 (5)
$[M + Na - H_2O - 2H]^-$	315 (8)	315 (12)	315 (12)	315 (8)
$[M - H]^-$	311 (1)	311 (3)	311 (3)	311 (2)
$[M - H_2O - H]^-$	293 (55)	293 (100)	293 (52)	293 (100)
$[M - H_2O - CO_2 - H]^-$	249 (8)	249 (9)	249 (3)	249 (7)
$[M - H_2O_2 - CO_2 - H]^-$	233 (4)	233 (3)	233 (2)	233 (2)
$[M - CH_3(CH_2)_2CHCH_2 - H_2O - H]^-$	223 (5)		223 (39)	
$[M - CH_3(CH_2)_2CHCH_2 - H_2O - CO - H]^-$	195 (22)		195 (44)	
$[M - CH_3(CH_2)_2CHCH_2 - H_2O - CO_2 - H]^-$	179 (11)		179 (18)	
$[M - CH_3CH_2(CH_2)_5COOH - H]^-$	167 (14)	167 (7)	167 (15)	167 (14)
	139 (14)	139 (6)	139 (14)	139 (5)
	113 (100)		113 (100)	
		197 (22)		197 (25)
		185 (75)		185 (72)
$[M - CH_3(CH_2)_4CHCHCCH - H_2O - H]^-$		171 (8)		171 (7)
		149 (17)		149 (14)
$[M - CH_3(CH_2)_4CHCHCCH - H_2O - H_2CO - H]^-$		141 (15)		141 (11)
$[M - CH_3(CH_2)_4CHCHCCH - H_2O - HCO_2H - H]^-$		125 (51)		125 (49)
$[CH_3(CH_2)_4CHCHCHCH_2 - H]^-$		123 (20)		123 (15)

[a]Abundances for cone voltage −50 V are given in parentheses.

13-regioisomers. Their maximal absorption wavelengths in diode array detection were found to be, respectively, 236 and 232 nm. Last, the co-elution of HPODE1 with an authentic standard of 13(*S*)-hydroperoxy-(9*Z*,11*E*)-octadecadienoic acid allowed to assign HPODE3 as 13-hydroperoxy-(9*E*,11*E*)-octadecadienoic acid. In the case of HPODE2 and 4, characteristic product ions were detected at *m*/*z* 197, 185 and 171. The latter ion resulted from the fission between C9 and C10 and subsequent elimination of water. Decarbonylation and decarboxylation led to the production of typical ions at *m*/*z* 141 and 125. These 9-regioisomers were further assigned based on their UV maximal absorption wavelengths. HPODE2 (λ_{max} 236 nm) appears as 9-hydroperoxy-(10*E*,12*Z*)-octadecadienoic acid while HPODE4 (λ_{max} 232 nm) is 9-hydroperoxy-(10*E*,12*E*)-octadecadienoic acid.

3.2. Structures of the HODE products

The separation of the 4 HODE could not be fully achieved in the selected chromatographic system. Peaks 1 and 3 could be assigned by mass spectrometry (Table 2). In addition, peak 1 co-eluted with an authentic standard of 13(*S*)-hydroxy-(9*Z*,11*E*)-octadecadienoic acid. Mass spectra of peaks 1 and 3 revealed parent ions at *m*/*z* 295 for $[M - H]^-$ and 317 for $[M + Na - 2H]^-$. Dehydration led to *m*/*z* 277. Characteristic fragments at *m*/*z* 171 and 123 were obtained from scission between

Table 2
Product ions (*m*/*z*) and proposed structures for fragments issued from hydroxyoctadecadienoic acids (HODE) in ESI–MS[a]

	HODE1 13-*Z*,*E*-HODE	HODE3 9-*E*,*E*-HODE
$[M + Na - 2H]^-$	317 (2)	317 (1)
$[M - H]^-$	295 (100)	295 (56)
$[M - H_2O - H]^-$	277 (42)	277 (100)
$[M - CO_2 - H]^-$	251 (2)	251 (1)
$[M - H_2O - CO_2 - H]^-$	233 (1)	233 (2)
$[M - CH_3(CH_2)_4CHO - H]^-$	195 (77)	
$[M - CH_3(CH_2)_2CHCH_2 - HCO_2H - H]^-$	179 (6)	
$[M - CH_3(CH_2)_4CHCHCHCH_2 - H]^-$		171 (100)
$[M - HCO(CH_2)_7CO_2H - H]^-$		123 (10)
	113 (13)	

[a]Abundances for cone voltage −50 V are given in parentheses.

Table 3
^{1}H NMR spectral data for regioisomeric 9- and 13-oxooctadecadienoic acids[a]

Compound	H_α	H_β	H_δ	H_γ	CH_2–CO	CH_2–C=C
13-*Z*,*E*-KODE	6.19 d (15.2)	7.50 dd (11.5, 15.2)	6.12 dd (11.5, 10.4)	5.91 dt (8.3, 10.4)	2.54 t (7.2), 2.35 t (7.5)	2.30 m
13-*E*,*E*-KODE	6.08 d (15.4)	7.13 dm (15.4)	6.14–6.18 m	6.14–6.18 m	2.53 t (7.4), 2.35 t (7.5)	2.17 m
9-*E*,*Z*-KODE	6.16 d (15.3)	7.49 ddd (0.7, 11.4, 15.3)	6.12 dd (11.4, 10.9)	5.91 dt (8.0, 10.9)	2.55 t (7.4), 2.34 t (7.5)	2.30 m
9-*E*,*E*-KODE	6.07 d (15.5)	7.13 dm (15.5)	6.15–6.19 m	6.15–6.19 m	2.53 t (7.4), 2.33 t (7.5)	2.17 m

[a]Chemical shift in ppm, multiplicity (coupling constant in Hz). Numbering is as follows: CO–CH_α=CH_β–CH_δ=CH_γ. Common chemical shifts as follows: 1.63 (m, 4H), 1.43 (m, 2H), 1.32 (m, 10H), 0.88 (t, 3H, 7.0 Hz).

C9 and C10 for peak 3. Presence of a maximal absorption at 232 nm led to the assignment of peak 3 as 9-hydroxy-(10*E*,12*E*)-octadecadienoic acid. Typical ions displayed by 13-hydroxy-(9*Z*,11*E*)-octadecadienoic acid (λ_{max} 234 nm) are *m*/*z* 195, 179 and 113. Ion at *m*/*z* 195 may result from bond cleavage between C12 and C13 while cleavage between C13 and C14 followed by a deformylation may lead to *m*/*z* 179.

Peak 2 is indeed a mixture of 13-hydroxy-(9*E*,11*E*)-octadecadienoic acid (λ_{max} 232 nm) and 9-hydroxy-(10*E*,12*Z*)-octadecadienoic acid (λ_{max} 234 nm) as revealed from UV and mass probing.

3.3. Structures of the KODE products

KODE1 exhibited a UV max at 280 nm. ^{1}H NMR of the ethylenic region displayed a dd at 7.50 ppm with *J* = 11.5, 15.2 Hz assigned to H11 (Table 3). At 5.91 ppm, H9 appeared as a dt (*J* = 8.3, 10.4 Hz). At, respectively, 6.19 and 6.12 ppm the splitting patterns were a d (*J* = 15.2 Hz, H12) and a dd (*J* = 11.5, 10.4 Hz, H10). Coupling constants of 10 and 15 Hz pointed to *cis* and *trans* geometries for the two ethylenic moieties suggesting that KODE1 is 13-oxo-(9*Z*,11*E*)-octadecadienoic acid. These results are in agreement with chemical shifts (Napolitano et al., 2002) and coupling constants obtained for 13-oxo-(9*Z*,11*E*)-octadecadienoic acid (Iacazio, 2003) or for the corresponding methyl ester (Kuklev et al., 1997; Hidalgo et al., 1992). Discrepancies are observed with other literature results (Chudinova et al., 1995; Dong et al., 2000). In particular, the lack of use of multiplicity led to inversion in proton assignments (Bull and Bronstein, 1990; Blackburn et al., 1997).

With KODE2, the most downfield proton at 7.13 ppm is part of an ABMX spin system from which a coupling constant of 15.4 Hz could be extracted. It was assigned to H11. A d (*J* = 15.4 Hz) was observed for the other ethylenic proton assigned as H12. The configuration of the double bond alpha to the carbonyl group is thus *trans*. KODE2 is ascribed to 13-oxo-(9*E*,11*E*)-octadecadienoic acid owing to a shorter absorption maximum (276 nm) compared to KODE1. Chemical shifts are consistent with those published previously (Bull and Bronstein, 1990).

KODE3 presented a UV max at 280 nm. Four well resolved signals were observed in the ^{1}H NMR ethylenic region. The most deshielded proton H11 appeared as a ddd at 7.49 ppm with a large *J* value of 15.3 Hz indicating a *trans* configuration for the double bond. At 5.91 ppm, a dt (*J* = 8.0, 10.9 Hz) was expected for H13 pointing to a *cis* geometry for the second unsaturation. A d at 6.16 ppm (*J* = 15.3 Hz, H10) and a dd (*J* = 11.4, 10.9 Hz, H12) confirmed the assignment of KODE3 as 9-oxo-(10*E*,12*Z*)-octadecadienoic acid (Iacazio, 2003; Kuklev et al., 1997).

The ethylenic region for KODE4 exhibited three distinct patterns: a dm at 7.13 ppm, part of an ABMX system (*J* = 15.5 Hz) and assigned to H11, a multiplet at 6.15–6.19 ppm for H12 and H13 and a d (*J* = 15.5 Hz) at 6.07 ppm for H10. Finally, a COSY revealed strong correlations between H10 and H11, H11 and the multiplet common to H12 and H13 but no correlation between H10 and both H12 and H13. Additional correlations were observed between the allylic methylene at 2.17 ppm and both H12 and H13 and more weakly with H11. Last, correlations were displayed between methylenes α (2.33 and 2.53 ppm) and β (1.63 ppm) to the different carbonyl groups. With a maximal absorption at 276 nm, KODE4 corresponds to 9-oxo-(10*E*,12*E*)-octadecadienoic acid (Kawagishi et al., 2002). Moreover, chemical shifts reported in pyridine for the ethylenic protons of the four KODE show a downfield move compared to those in chloroform (Watanebe et al., 1999). Last, equilibration of a mixture of the four KODE in the presence of iodine led to isomerization to all-*trans* KODE2 and 4.

All KODE presented common fragments in their negative ESI mass spectra (Table 4). Parent ions were detected at *m*/*z* 293. A low abundance of sodium adducts was also observed at *m*/*z* 315. Decarboxylation led to *m*/*z* 249. Furthermore, 13-regioisomers displayed characteristic fragments at *m*/*z* 195 and 179 resulting from bond scission between C13 and C14 followed by either decarbonylation or decarboxylation. Successive

Table 4
Product ions (*m*/*z*) and proposed structures for fragments issued from oxooctadecadienoic acids (KODE) in ESI–MS[a]

	KODE1 13-*Z*,*E*-KODE	KODE2 13-*E*,*E*-KODE	KODE3 9-*E*,*Z*-KODE	KODE4 9-*E*,*E*-KODE
$[M-H]^-$	293 (100)	293 (100)	293 (100)	293 (100)
$[M-CO_2-H]^-$	249 (8)	249 (8)	249 (3)	249 (3)
$[M-CH_3(CH_2)_4CHCH_2-H]^-$			197 (11)	197 (9)
$[M-CH_3(CH_2)_2CHCH_2-CO-H]^-$	195 (16)	195 (10)		
			185 (37)	185 (37)
$[M-CH_3(CH_2)_2CHCH_2-CO_2-H]^-$	179 (13)	179 (5)		
			149 (5)	149 (5)
$[M-CH_3(CH_2)_2CHCH_2-CO-CH_2CH_2-H]^-$	167 (13)	167 (12)		
$[M-CH_3(CH_2)_4(CHCH)_2CHO-H]^-$			141 (5)	141 (6)
$[M-CH_3(CH_2)_2CHCH_2-CO-2xCH_2CH_2-H]^-$	139 (6)	139 (3)		
$[M-CH_3(CH_2)_4CHCHCHCH_2-CO_2-H]^-$			125 (20)	125 (18)
$[CH_3(CH_2)_4CHCHCHCH_2-H]^-$	113 (82)	113 (76)	123 (5)	123 (4)
	113 (82)	113 (76)		

[a] Abundances for cone voltage −50 V are given in parentheses.

fragmentations of ion 195 led to characteristic ions at *m*/*z* 167, 139 and 113 resulting from the loss of ethylene or CO. Typical ions for 9-ketodienes were detected at *m*/*z* 197, 185, 149, 141, 125 and 123. Cleavage between C11 and C12 may result in *m*/*z* 197 while cleavage between C9 and C10 may produce *m*/*z* 123.

3.4. Peroxidation of HSA-bound linoleic acid

The course of the peroxidation of HSA-bound linoleic acid was followed by RP-HPLC (Fig. 1). The peroxidation products HPODE, HODE and KODE as well as remaining LH were quantified by peak area according to the calibrations with 13(*S*)-(10*Z*,12*E*)-HPODE, 13(*S*)-(10*Z*,12*E*)-HODE, a synthetic sample of KODE and LH. During the first 7 h of reaction, HSA-bound linoleic acid was mainly converted into the primary oxidation product HPODE and secondary oxidation products HODE and KODE (Fig. 2). Levels in KODE were found to be substantial whereas HODE appeared as minor degradation products in the albumin system. Additionally, the mass balance is consistent with HPLC chromatograms showing no further degradation products during this period. The values for the extraction yields and calibration factors are thus confirmed.

Major differences were displayed in the accumulation of the four HPODE isomers (Fig. 3). Similar concentrations in 13- and 9-(*E*,*E*)-HPODE were observed after 7 h of reaction whereas 13-(*Z*,*E*)- and 9-(*E*,*Z*)-HPODE accumulated to a lesser extent. The trend observed at 7 h was confirmed by the data collected between 24 and 30 h of reaction. The most intriguing behavior was displayed by 9-(*E*,*Z*)-HPODE whose concentration peaked at 6 h and then decreased. For KODE, rates appeared to differ appreciably for the various isomers with a predominant production of 9-(*E*,*E*)-KODE (Fig. 4). In addition, higher levels in *E*,*E*-stereoisomers were formed compared to the *Z*,*E*-ones. At the end of the reaction the following order of accumulation was observed: 9-(*E*,*E*)-KODE > 13-(*E*,*E*)-KODE > 13-(*Z*,*E*)-KODE > 9-(*E*,*Z*)-KODE. With HODE, this analysis is partly prevented owing to the lack of product separation. The peak for 9-(*E*,*E*)-HODE was however integrated as twice the area of the shoulder on the left side of the peak for 13-(*Z*,*E*)-HPODE. Differences are again outlined: 13-(*Z*,*E*)-HODE was slightly formed whereas 9-(*E*,*Z*)-HODE and 13-(*E*,*E*)-HODE accumulated almost linearly (Fig. 5). The trend for 9-(*E*,*E*)-HODE should be viewed with care because of a high similitude with that observed for 13-(*Z*,*E*)-HPODE.

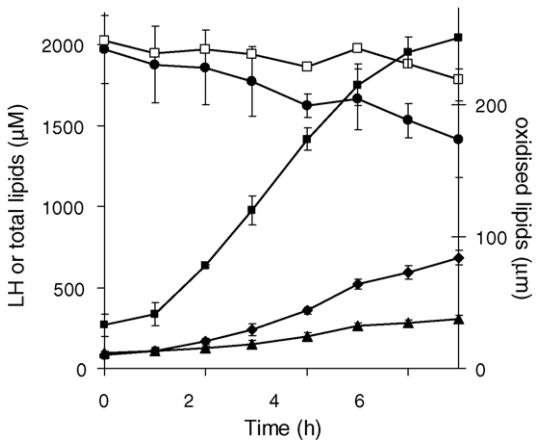

Fig. 2. Accumulation of HPODE (■), KODE (♦), HODE (▲) during the course of the peroxidation of HSA-bound linoleic acid (●) at 37 °C. Total lipids (□) are the sum of oxidized lipids and LH ($n = 4$).

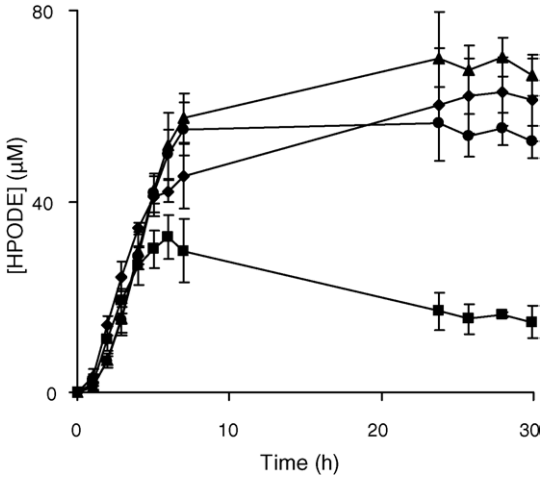

Fig. 3. Formation of the different HPODE regioisomers during the course of the peroxidation of HSA-bound linoleic acid: 13-(*E*,*E*)-HPODE (▲), 13-(*Z*,*E*)-HPODE (♦), 9-(*E*,*E*)-HPODE (●) and 9-(*E*,*Z*)-HPODE (■).

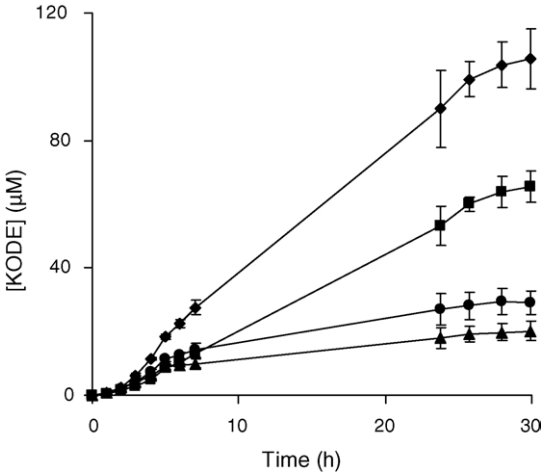

Fig. 4. Formation of the different KODE regioisomers during the course of the peroxidation of HSA-bound linoleic acid. 9-(*E*,*E*)-KODE (♦), 13-(*E*,*E*)-KODE (■), 13-(*Z*,*E*)-KODE (●) and 9-(*E*,*Z*)-KODE (▲).

4. Discussion

Negative ESI–MS provided sufficient information for identification of classes of oxidation products in the peroxidation of HSA-bound linoleic acid. At −20 V, parent ions were mainly obtained for KODE and HODE while HPODE displayed a dehydrated form of the parent ion. In addition, negative ESI–MS proved to be a valuable tool for determining the position of oxygenation in the 9- and 13-regioisomers of the oxidation products derived from linoleic acid. At the higher voltage of −50 V, common characteristic ions at *m*/*z* 195, 179 and 113 are revealed

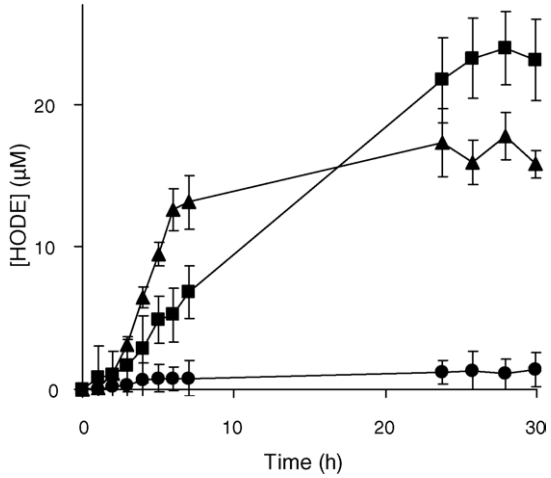

Fig. 5. Formation of the different HODE regioisomers during the course of the peroxidation of HSA-bound linoleic acid: 9-(*E*,*Z*)-HODE + 13-(*E*,*E*)-HODE (■), 9-(*E*,*E*)-HODE (▲) and 13-(*Z*,*E*)-HODE (●).

for all 13-regioisomers while 9-regioisomers share a fragment ion at *m*/*z* 123. Furthermore, almost identical spectra to those obtained in this work were obtained by collision-induced decomposition of the molecular ions for 9- and 13-HPODE in the negative mode (MacMillan and Murphy, 1995). This emphasizes that routinely available LC–ESI–MS can be used for the characterization of these oxygenated products. Characteristic ions at *m*/*z* 113 from 13-regioisomers and *m*/*z* 185 from 9-regioisomers appear to result from an apparent cleavage of the double bond adjacent to the oxygenated center. A mechanism involving a 1,5 sigmatropic proton shift was suggested for the formation of these fragments (MacMillan and Murphy, 1995).

Attempts in positive ESI–MS proved to be less successful. At low voltage, no single ion prevails. The parent ions mainly appear as sodium and/or acetonitrile adducts coexisting with the dehydrated forms, respectively, $[M - H_2O + H]^+$ for HODE and KODE and $[M - H_2O_2 + H]^+$ for HPODE. At higher voltages, an elevated proportion of triply unsaturated aliphatic fragments was detected indicating easy cleavages of the ions in these conditions. The use of ammonium acetate in the HPLC solvent system did not improve the response in the KODE mass. Characteristic ions of the 9- or 13-regiochemistry were also found although in a lower abundance than in the negative mode (Schneider et al., 1997). As a matter of fact, the negative mode in ESI–MS is the most valuable as it provides clean molecular ions at low voltages as well as several characteristic fragments of the 9- and 13-oxygenated products at higher voltages.

We also report a full characterization of the different KODE isomers in the same ^{1}H NMR conditions. Identical spectra were obtained for both *E*,*E*-isomers, on one hand, and *Z*,*E*-isomers on the other hand, reflecting the isolation of the structural moiety in the hydrocarbon chain. The main differences were linked to the stereochemistry of the double bond δ to the keto group. Chemical shifts for olefinic and allylic protons were thus found to be characteristic of the *E*,*E*- and *Z*,*E*-stereochemistries.

Long chain fatty acids (LCFA, C16–C20) are crucial intermediates in the lipid metabolism. The non-esterified forms of fatty acids are not soluble in plasma and are thus transported by albumin (Peters, 1996). Up to seven binding sites for LCFA have been located in human albumin with affinities in the 10^7 to $10^8\ M^{-1}$ range (Petitpas et al., 2001). Because the total concentration of LCFA is just below 1 mM in plasma and that of albumin is about 0.6 mM, circulating albumin typically carries 1–2 LCFA molecules. This number may rise to about 4 LCFA per HSA after strenuous exercise or other adrenergic stimulation (Peters, 1996). In our study, HSA was bound with four molecules of linoleic acid and placed next in oxidizing conditions. The thermal decomposition of lipid peroxidation initiator AAPH delivers peroxyl radicals at a constant rate (Niki, 1990). The accumulation in time of the peroxidation products as well as the consumption of LH was followed by reverse-phase HPLC. Although the full separation of the primary and secondary products of linoleic acid cannot be achieved in this chromatographic system, their quantification remains feasible. Absorption of hydroxy- and hydroperoxyoctadecadienoic acids extends from 210 to 260 nm while that of the corresponding ketodiene is in the range 250–310 nm. Quantitative analysis was performed for concentrations 1–250 μM in a single oxidation product without any undesirable overlap for detection at 234 and 280 nm. During the first hour of reaction, the levels in peroxidation products remain low suggesting an antioxidant activity of albumin. When the protection of HSA-bound linoleic acid is over, HPODE, HODE and KODE accumulate at a nearly linear rate. After 7 h of reaction, measured concentrations were found to be 251 μM for HPODE, 84 μM for KODE and 37 μM for HODE. In the presence of albumin, hydroperoxides appear as the major peroxidation products followed by ketodienes and finally hydroxides. Beyond this time, the rate in HPODE levels off while the secondary oxidation products keep accumulating supporting the conversion of HPODE in HODE and KODE. Furthermore, the HPLC profile displays the formation of compounds with shorter retention times indicating cleavages in the accumulated primary or secondary oxidation products.

In a homogeneous system, lipid peroxidation yields a 13-HPODE/9-HPODE ratio of one. In the presence of albumin, this ratio was found to increase steadily to end up at 1.8 after 30 h of reaction. The 13- to 9-regioselectivity induced by HSA probably results from the location of the linoleic acid molecules in their tunnel-like binding sites. ESR studies have shown that the tightest restriction in the binding channel is between C5 and C13–15 (Peters, 1996). Because the dienyl moiety is located in this area, steric hindrance may favor the addition of oxygen on the 13-position rather than the 9-position of the pentadienyl radical issued from linoleic acid ($L^{\bullet} + O_2 \rightarrow LOO^{\bullet}$). In contrast, a 9-regioselectivity was observed for the KODE formation in the presence of HSA. The lower stability of the 9-HPODE may result in an accelerated conversion to the 9-KODE regioisomers. The presence of HSA during lipid peroxidation favors the formation of thermodynamically more stable *E*,*E*-stereoisomers. The reversible addition of oxygen onto the pentadienyl radical may be controlled by HSA, thus favoring the *E*,*E*-stereoisomers. Moreover, the conversion of HPODE to KODE (formally a dehydration) may involve a double-bond rearrangement to produce the thermodynamically more stable *E*,*E*-KODE.

5. Conclusion

An efficient RP-HPLC method was developed for the detection of primary and secondary peroxidation products issued from oxidation of linoleic acid bound to human serum albumin. Diode array detection allowed the quantification of all the regioisomeric KODE and HPODE as single compounds while the four HODE isomers were resolved as three peaks. Full characterization by ESI–MS and NMR was conducted revealing a 13- versus 9-regioselectivity for the peroxidation step in this plasma model. Furthermore, unstable 9-(*E*,*Z*)-HPODE decayed rapidly to give major KODE isomer, 9-(*E*,*E*)-KODE. The favored formation of thermodynamically controlled *E*,*E*-stereoisomers was also observed for both HPODE and KODE. Mechanisms involved in the regio- and stereoselectivities of the peroxidation of HSA-bound linoleic acid will be discussed more deeply elsewhere.

Acknowledgement

We thank Dr. Robert Faure (Spectropole, Marseille, France) for help in NMR determination.

References

Banni, S., Contini, M.S., Angioni, E., Deiana, M., Dessi, M.A., Melis, M.P., Carta, G., Corongiu, F.P., 1996. A novel approach to study linoleic acid autoxidation: importance of simultaneous detection of the substrate and its derivative oxidation products. Free Radic. Res. 25, 43–53.

Blackburn, M.L., Ketterer, B., Meyer, D.J., Juett, A.M., Bull, A.W., 1997. Characterization of the enzymatic and nonenzymatic reaction of 13-oxooctadecadienoic acid with gluthatione. Chem. Res. Toxicol. 10, 1364–1371.

Bull, A.W., Bronstein, J.C., 1990. Production of unsaturated carbonyl compounds during metabolism of hydroperoxy fatty acids by colonic homogenates. Carcinogenesis 11, 1699–1704.

Bylund, J., Ericsson, J., Oliw, E.H., 1998. Analysis of cytochrome P450 metabolites of arachidonic and linoleic acids by liquid chromatography–mass spectrometry with ion trap MS2. Anal. Biochem. 265, 55–68.

Chan, H.W.S., Levett, G., 1977. Autoxidation of methyl linoleate. Separation and analysis of isomeric mixtures of methyl linoleate hydroperoxides and methyl hydroxylinoleates. Lipids 12, 99–104.

Chudinova, V.V., Chudinov, M.V., Eremin, S.V., Alekseev, S.M., 1995. Preparative separation and ^{1}H NMR identification of products of linoleic acid autoxidation. Bioorg. Khim. 21, 545–553.

Dix, T.A., Marnett, L.J., 1985. Conversion of linoleic acid hydroperoxide to hydroxy, keto, epoxyhydroxy, and trihydroxy fatty acids by hematin. J. Biol. Chem. 260, 5351–5357.

Dong, M., Oda, Y., Hirota, M., 2000. (10*E*,12*Z*,15*Z*)-9-hydroxy-10,12,15-octadecatrienoic acid methyl ester as an anti-inflammatory compound from *Ehretia dicksonii*. Biosci. Biotechnol. Biochem. 64, 882–886.

Gardner, H.W., Grove, M.J., 2001. Method to produce 9(*S*)-hydroperoxides of linoleic and linolenic acids by maize lipoxygenase. Lipids 36, 529–533.

Hamberg, M., 1971. Steric analysis of hydroperoxydes formed by lipoxygenase oxygenation of linoleic acid. Anal. Biochem. 43, 515–526.

Hidalgo, F.J., Zamora, R., Vioque, E., 1992. Syntheses and reactions of methyl (*Z*)-9,10-epoxy-13-oxo-(*E*)-11-octadecenoate and methyl (*E*)-9,10-epoxy-13-oxo-(*Z*)-11-octadecenoate. Chem. Phys. Lipids 60, 225–233.

Hilbers, M.P., Finazzi-Agrò, A., Veldink, G.A., Vliegenthart, J.F.G., 1996. Purification and characterization of a lentil seedling lipoxygenase expressed in *E. coli*: implications for the mechanism of oxodiene formation by lipoxygenases. Int. J. Biochem. Cell Biol. 28, 751–760.

Iacazio, G., 2003. Easy access to various natural keto polyunsaturated fatty acids and their corresponding racemic alcohols. Chem. Phys. Lipids 125, 115–121.

Iwase, H., Takatori, T., Nagao, M., Nijima, H., Iwadate, K., Matsuda, Y., Kobayashi, M., 1998. Formation of keto and hydroxy compounds of linoleic acid in submitochondrial particles of bovine heart. Free Radic. Biol. Med. 24, 1492–1503.

Kawagishi, H., Miyazawa, T., Kume, H., Arimoto, Y., Inakuma, T., 2002. Aldehyde dehydrogenase inhibitors from the mushroom clitocybe clavipes. J. Nat. Prod. 65, 1712–1714.

Kerwin, J.L., Torvik, J.J., 1996. Identification of monohydroxy fatty acids by electrospray mass spectrometry and tandem mass spectrometry. Anal. Biochem. 237, 56–64.

Kuhn, H., Borchert, A., 2002. Regulation of enzymatic lipid peroxidation: the interplay of peroxidizing and peroxide reducing enzymes. Free Radic. Biol. Med. 33, 154–172.

Kuklev, D.V., Christie, W.W., Durand, T., Rossi, J.C., Vidal, J.P., Kasyanov, S.P., Akulin, V.N., Bezuglov, V.B., 1997. Synthesis of keto- and hydroxydienoic compounds from linoleic. Chem. Phys. Lipids 85, 125–134.

MacMillan, K.D., Murphy, R.C., 1995. Analysis of lipid hydroperoxides and long-chain conjugated keto acids by negative ion electrospray mass spectrometry. J. Am. Soc. Mass Spectrom. 6, 1190–1201.

Matthew, M.A., Chan, H.W., Galliard, T., 1997. A simple method for the preparation of pure 9-D-hydroperoxide of linoleic acid and methyl linoleate based on the positional specificity of lipoxygenase in tomato fruit. Lipids 12, 324–326.

Napolitano, A., Crescenzi, O., Camera, E., Giudicianni, I., Picardo, M., d'Ischia, M., 2002. The acid-promoted reaction of ethyl linoleate with nitrite. New insights from *N*-15-labelling and peculiar reactivity of a model skipped diene. Tetrahedron 58, 5061–5067.

Niki, E., 1990. Free radical initiators as source of water- or lipid-soluble peroxyl radicals. Meth. Enzymol. 186, 100–108.

Pérez Gilabert, M., Garcia Carmona, F., 2002. Chromatographic analysis of lipoxygenase products. Anal. Chim. Acta 465, 319–335.

Peters, T., 1996. All About Albumin. Academic Press, San Diego.

Petitpas, I., Grüne, T., Bhattacharya, A.A., Curry, S., 2001. Crystal structures of human serum albumin complexed with monounsaturated and polyunsaturated fatty acids. J. Mol. Biol. 314, 955–960.

Porter, N.A., Wujek, J.S., 1987. Allylic hydroperoxide rearrangement: β-scission or concerted pathway. J. Org. Chem. 52, 5085–5089.

Schneider, C., Schreier, P., Herderich, M., 1997. Analysis of lipoxygenase-derived fatty acid hydroperoxides by electrospray ionization tandem mass spectrometry. Lipids 32, 331–336.

Spiteller, P., Spiteller, G., 1998. Strong dependence of the lipid peroxidation product spectrum whether Fe^{2+}/O_2 or Fe^{3+}/O_2 is used as oxidant. Biochim. Biophys. Acta 1292, 23–40.

Spiteller, D., Spiteller, G., 2000. Oxidation of linoleic acid in LDL: an important event in atherogenesis. Angew. Chem. Int. Ed. 39, 585–589.

Watanebe, J., Kawabata, J., Kasai, T., 1999. 9-Oxooctadeca-10,12-dienoic acids as acetyl-CoA carboxylase inhibitors from red pepper (*Capsicum annuum* L.). Biosci. Biotechnol. Biochem. 63, 489–493.

Wu, Z., Robinson, D.S., Domoney, C., Casey, R., 1995. High-performance liquid chromatography analysis of the products of linoleic acid oxidation catalyzed by pea (*Pisum sativum*) seed lipoxygenases. J. Agric. Food Chem. 43, 337–342.